

# Unique features and fabrication of site-controlled Ge quantum dots / SiGe microdisk systems

Jia Yan, Ningning Zhang, Peizong Chen, Kun Peng, Zuimin Jiang and Zhenyang Zhong\*

State Key Laboratory of Surface Physics and Department of Physics, Fudan University, Shanghai 200438, People's Republic of China.

\*Corresponding author. E-mail: zhenyangz@fudan.edu.cn



## I. Abstract

A tunable and efficient silicon-based light source remains elusive now. Efficient coupling (a precise spatial and spectral overlap) to integrated high Q-factor cavities is crucial for the employment of germanium quantum dot emitters in future monolithic silicon-based optoelectronic platforms<sup>1-2</sup>. We find a feasible and creative route toward precise site-controlling of Ge QDs at microresonator by fabricating microcavities followed by growing ordered QDs on pit-patterned microdisks. The inherent mechanisms of these peculiarities are explained by the surface chemical potential distribution.

## II. Motivation

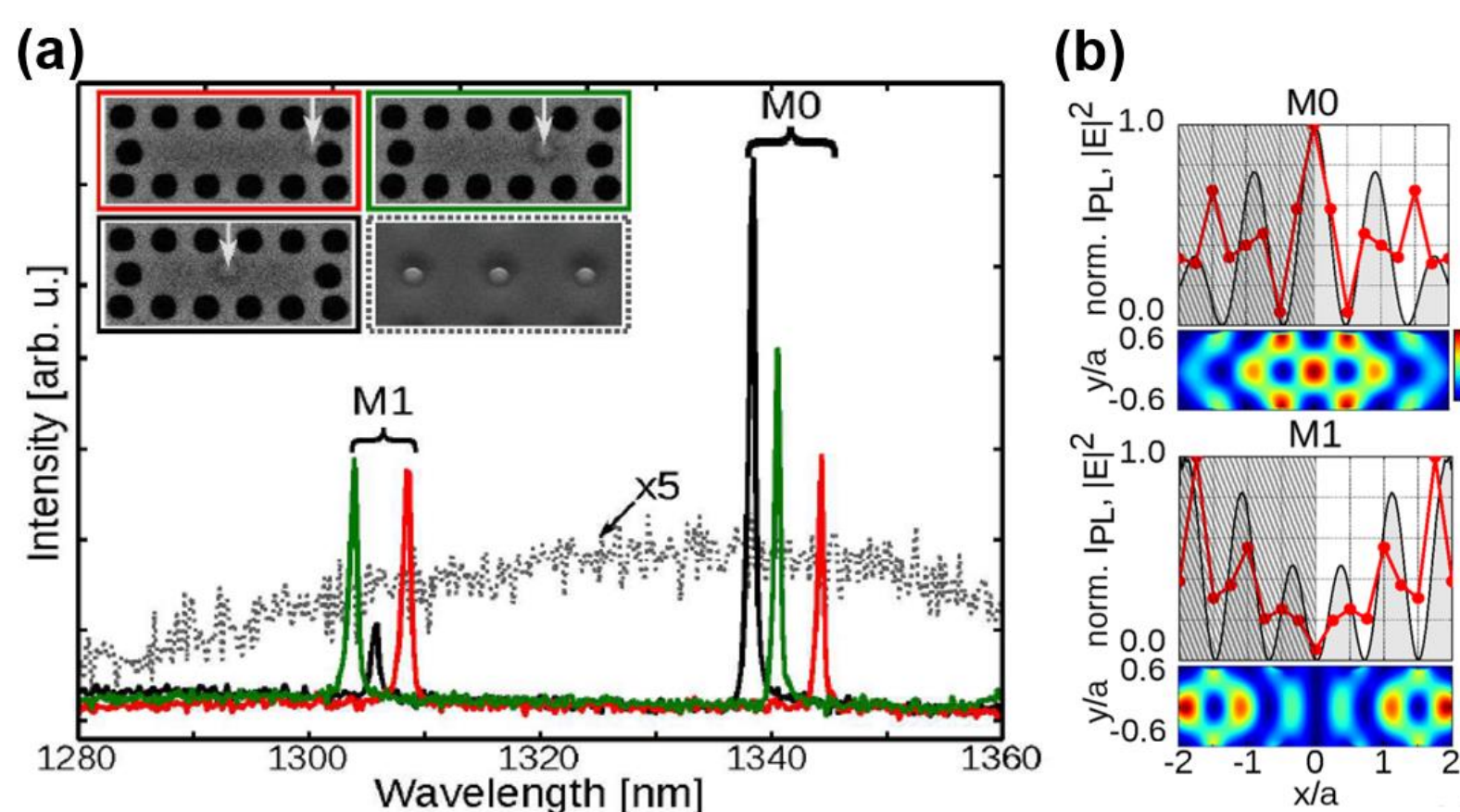


Fig 1. Photoluminescence spectra for a series of single quantum dots at varying positions within the photonic crystal cavity. (a) PL spectra of cavity modes M0 and M1. (b) The electric field energy distribution  $|E|^2$  for each mode.<sup>3</sup>

## III. Manufacturing process

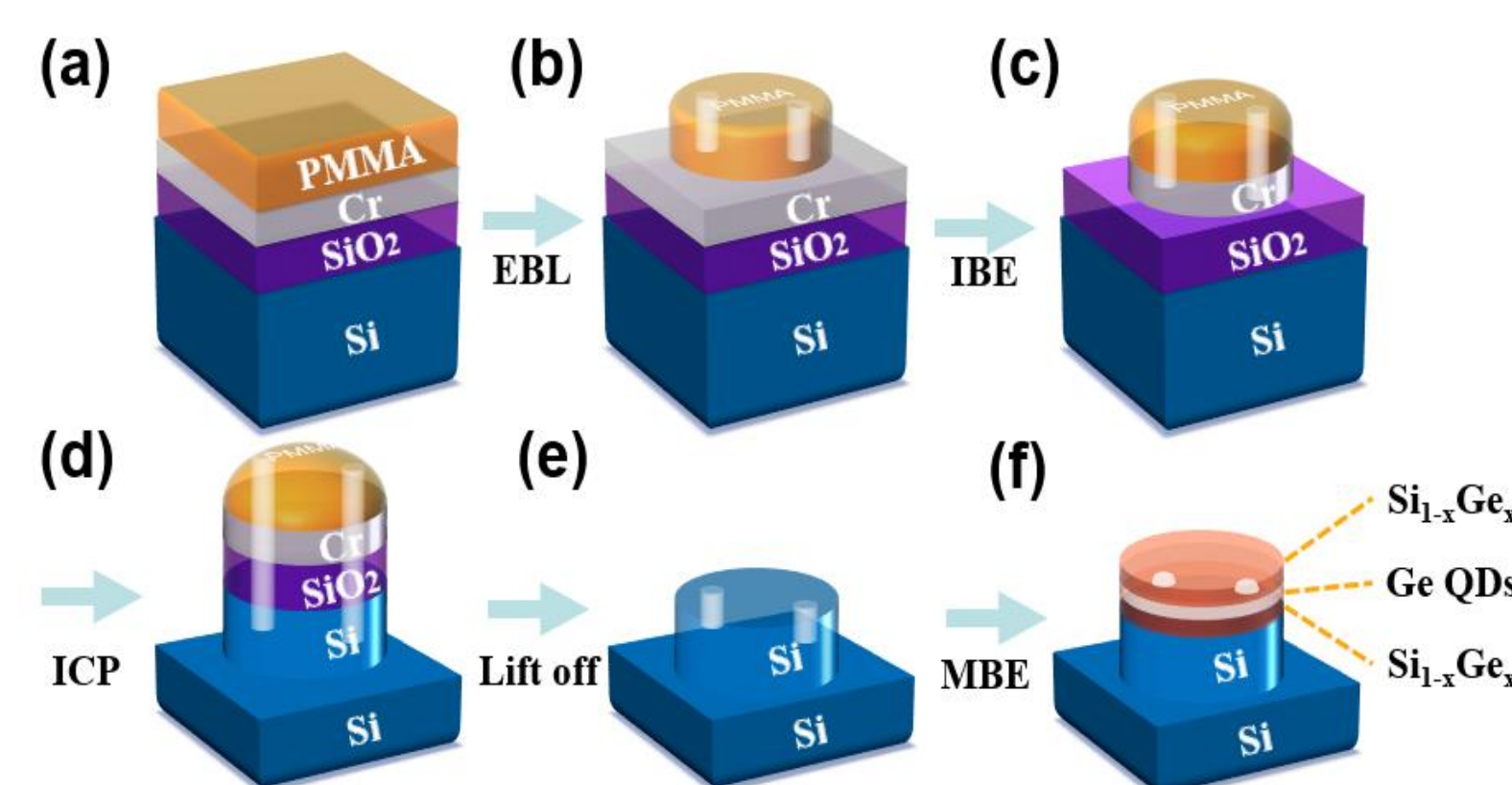


Fig 2. Process flow for pit-patterned optical cavities. The white columns represent portions that have been etched away.

## IV. Optical cavity design

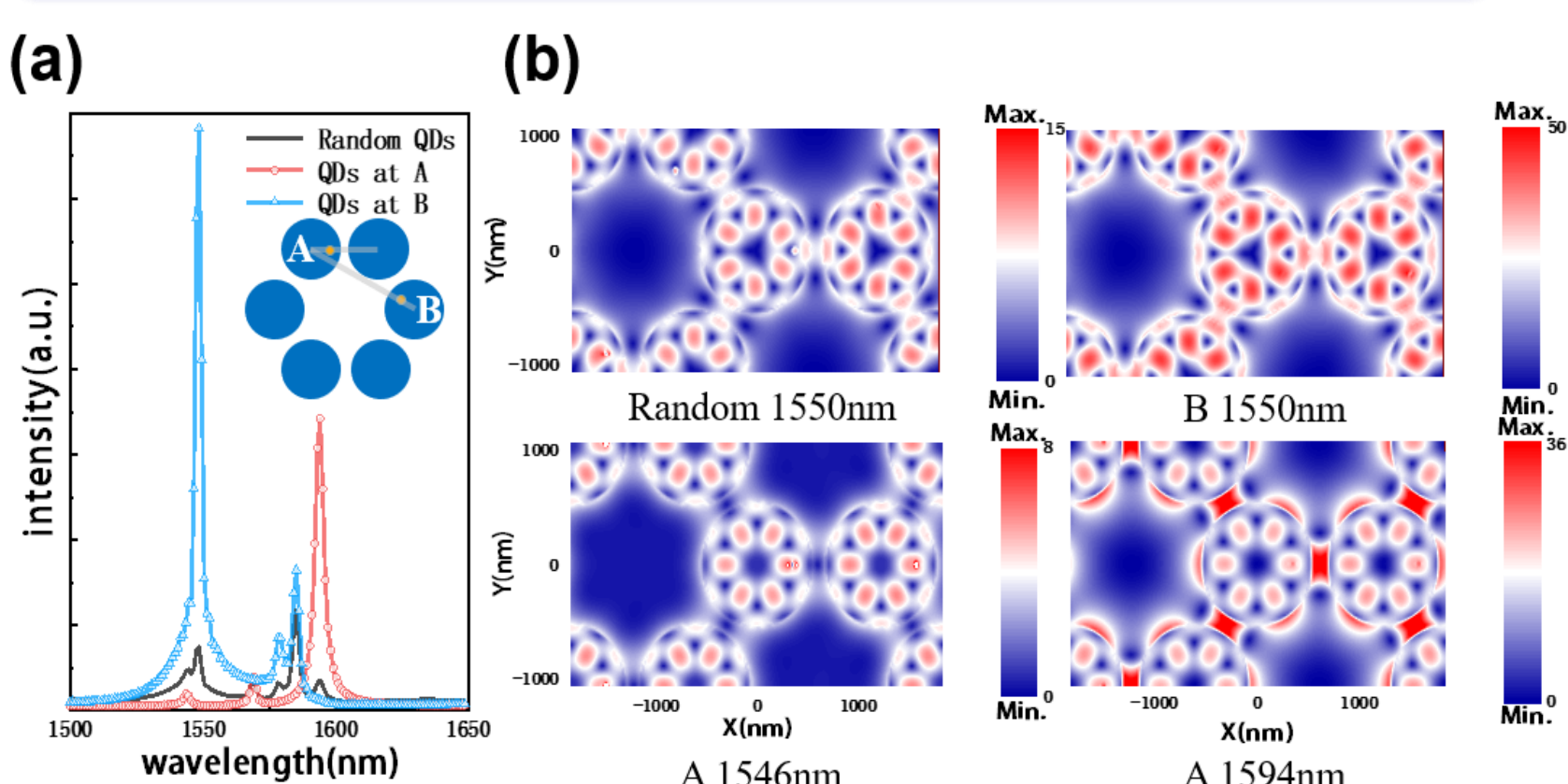


Fig 3. (a) Simulated spectra of the nanodisk arrays. The inset is schematic illustration of the models. The quantum dots A are located on the direct connection between the two microdisks while QDs B are off by 30 degrees. (b) The electric field (E) distribution for each mode in the XY plane.

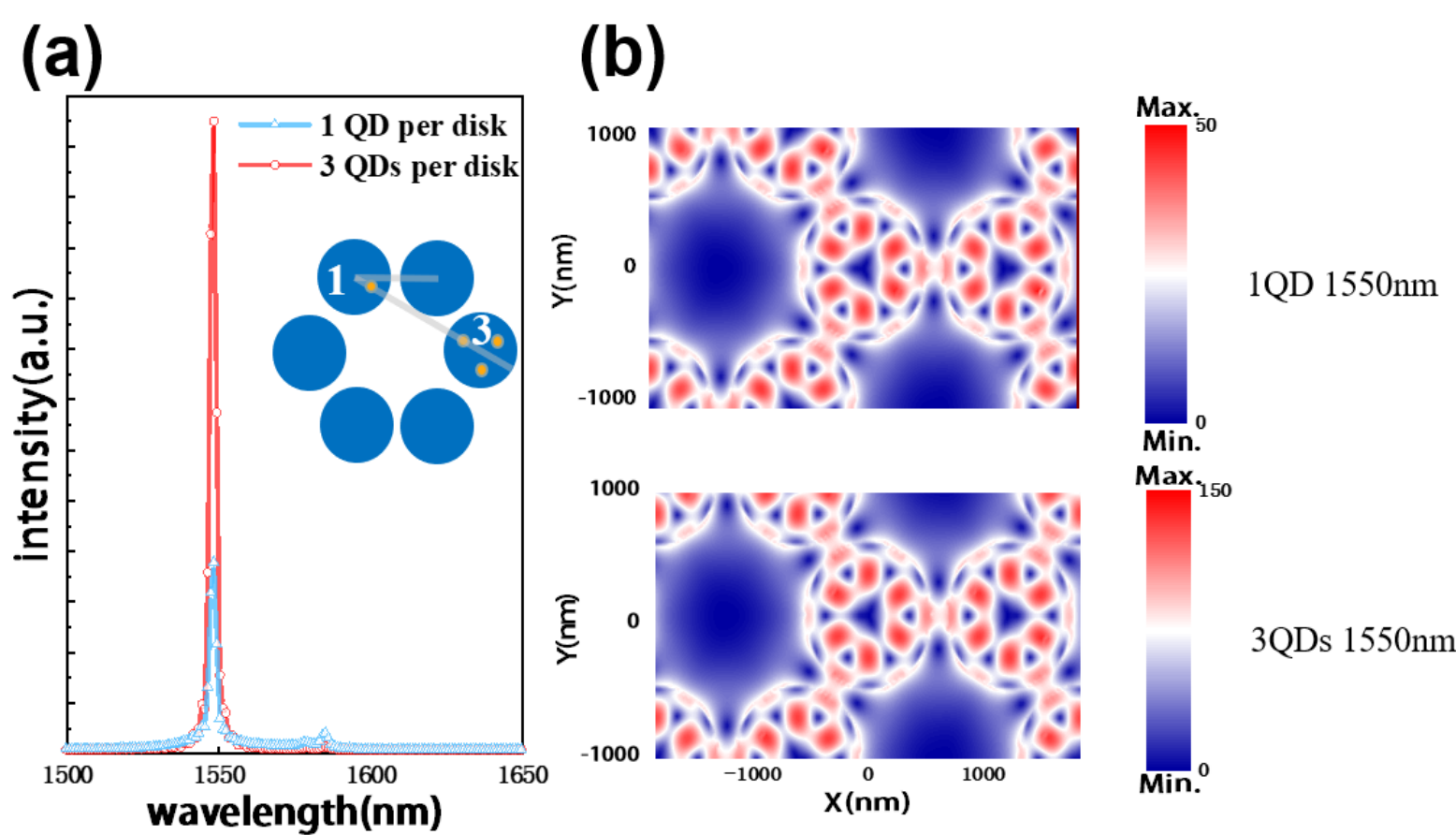


Fig 4. (a) Emission spectra of the honeycomb arrays. The inset is schematic illustration of different number of quantum dots. (b) The electric field (E) distribution for 1 or 3 QDs per disk in the XY plane at the communication wavelength.

## V. The Surface chemical potential model

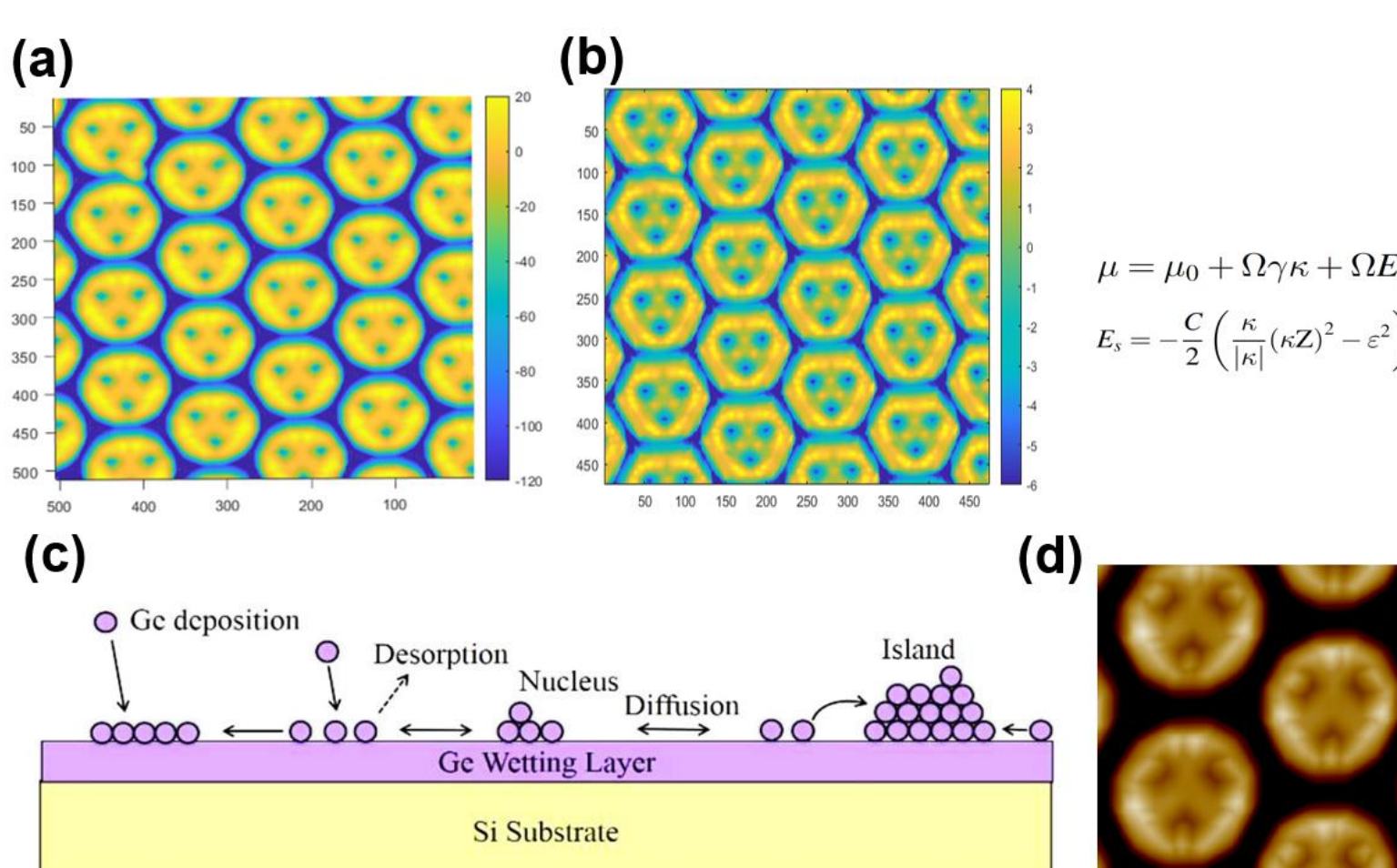


Fig 5. (a) Height distribution before growing quantum dots of hexagonal array (AFM). (b) Corresponding computed surface chemical potential distribution.  $E_s$  is the energy of strain relaxation energy,  $\mu$  means the surface curvature. (c) The heteroepitaxial growth modes of thin films. (d) Height distribution after Molecular Beam Epitaxy (MBE). The low chemical potential in the pits on the cavities results in site-controlling of Ge QDs.

## VI. The surface topography

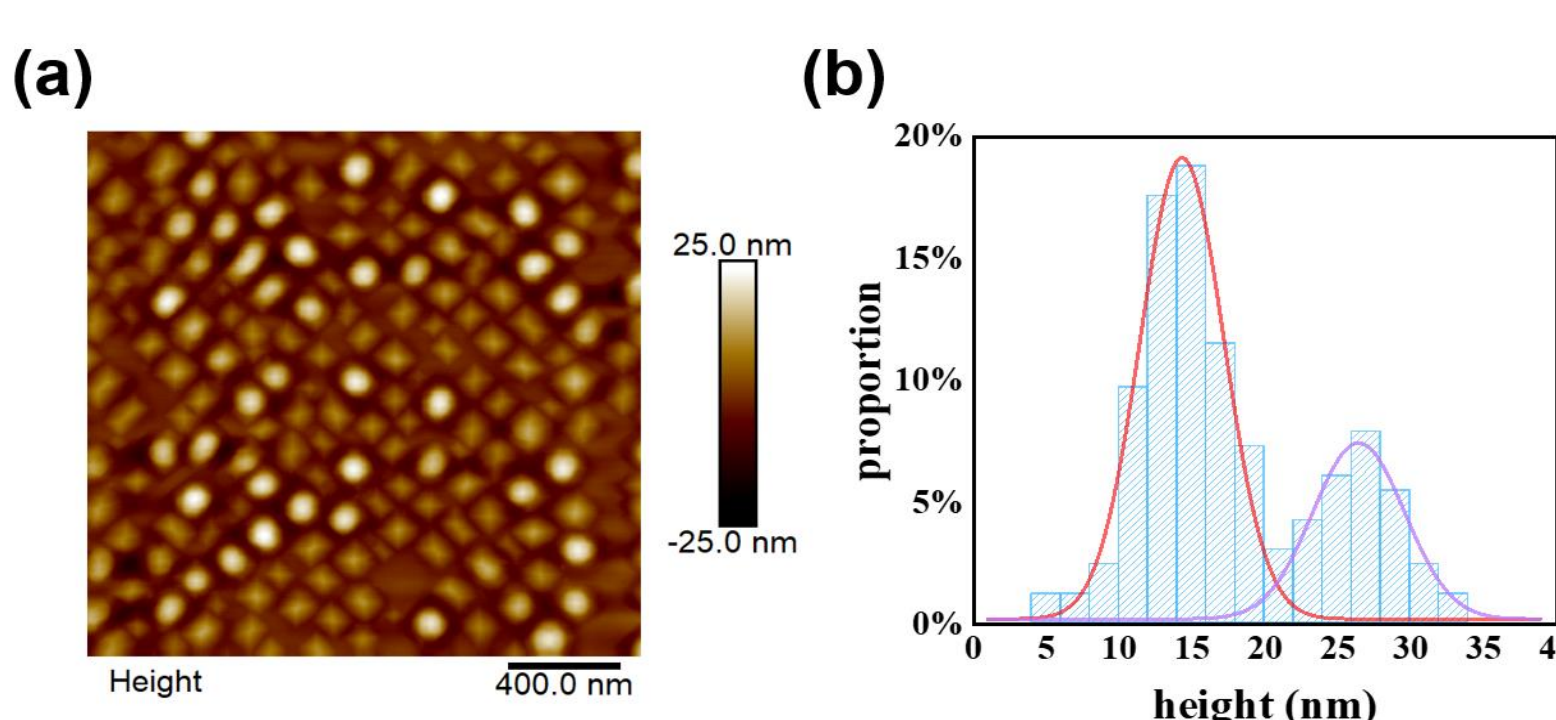


Fig 6. Morphologies and height distributions of Ge QDs of unpatterned region. (a) AFM Image ( $2 \times 2 \mu\text{m}^2$ ) and (b) Height distribution of QDs. There are two types of quantum dots: the pyramid ( $14.3 \pm 1.0 \text{ nm}$ ) and the dome ( $26.5 \pm 2.8 \text{ nm}$ ).

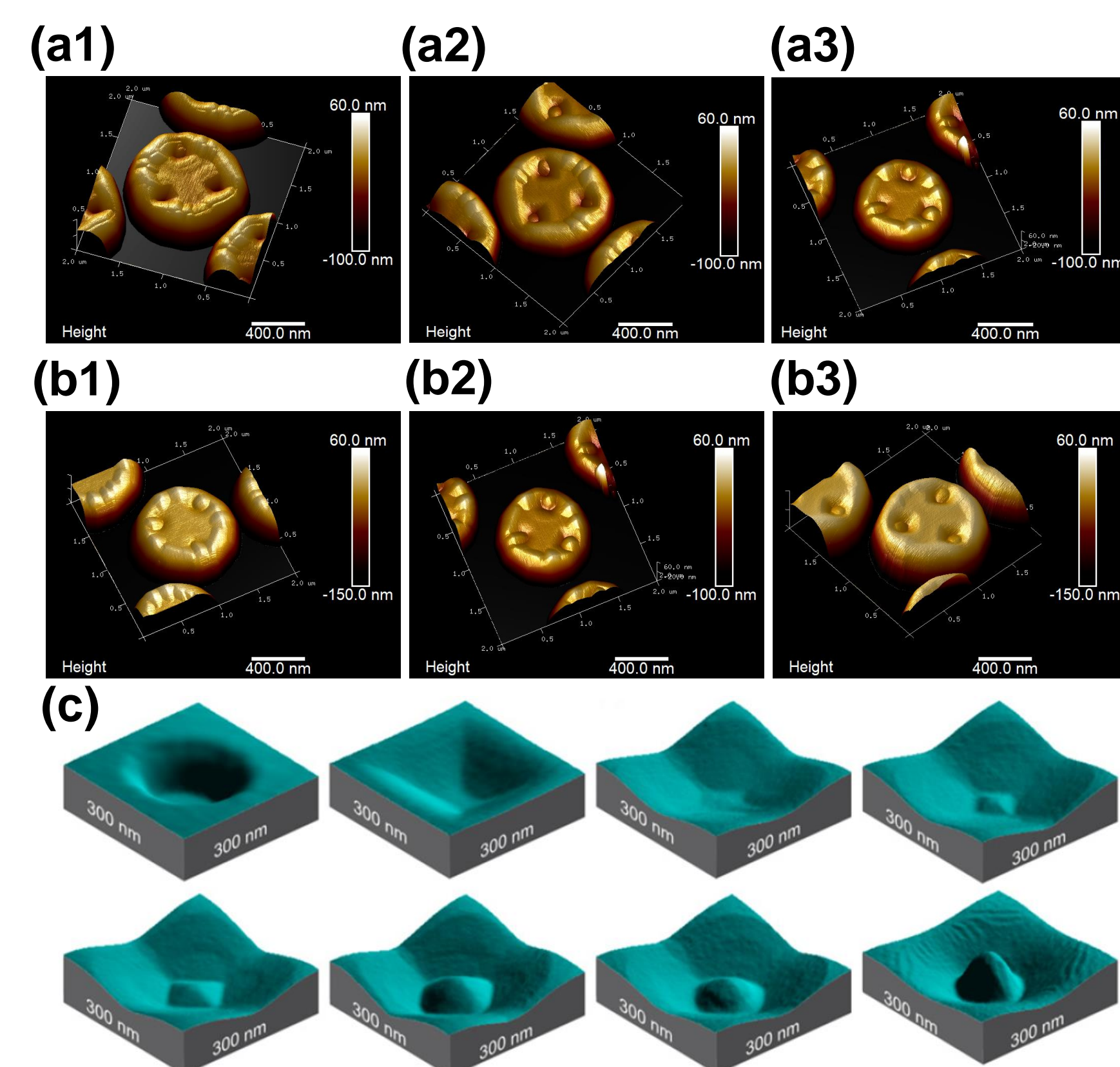


Fig 7. The change of surface morphology with the increase of (a) thickness of growth / (b) pit size. It is also imperative to select the appropriate growth temperature. (c) A animation diagram of growth procedure.

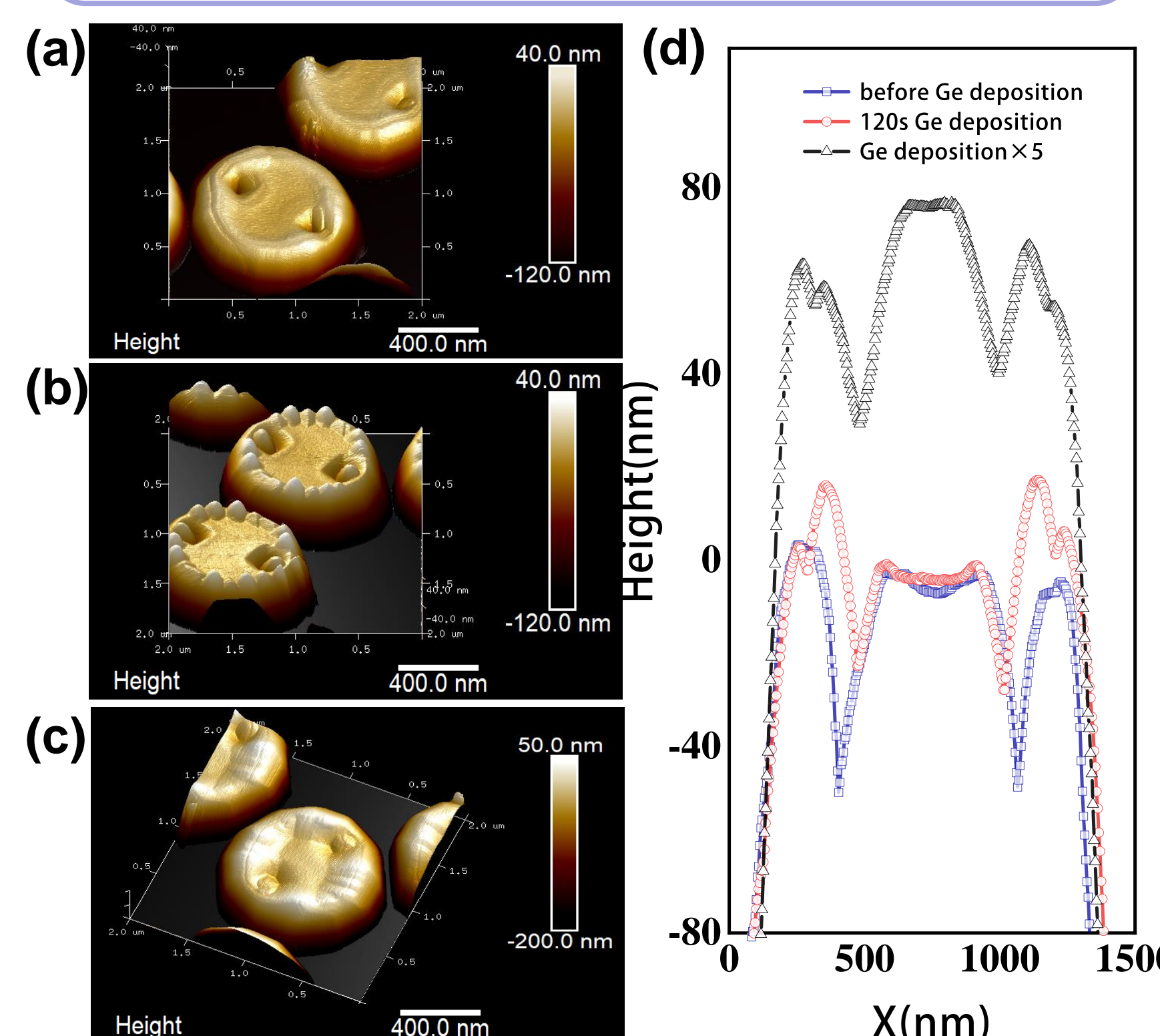


Fig 8. (a) Optical cavities array before Ge growth, (b) Monolayer germanium quantum dots were grown (The total amount of deposition is little more than the optimum one) (c) Multilayer QDs situation. (d) A cross section of several growing conditions.

[1] Bogaerts, W. Nature 586, 207-216 (2020).  
[2] Zhu, G. Scientific Reports 10, 253 (2020).  
[3] Magdalena. ACS Photonics 4(3): 665-673 (2017).

## VII. Conclusion

1. The epitaxial growth of Ge on SiGe microdisks results in the preferential growth of Ge QDs at the pits because the lower surface chemical potential. We achieve site-controlled Ge quantum dots .
2. The height and the linear density of Ge QDs can be tailored via the amount of deposited Ge and the size or number of the pits.
3. The intensity of emission of a certain WGM can be improved when the QDs only grow at field antinodes of the WGM, which will give rise to the actually strong light-mater interaction.